DOI: 10.1002/ejic.201001092

Diiron Complexes with Pendant Phenol Group(s) as Mimics of the Diiron Subunit of [FeFe]-Hydrogenase: Synthesis, Characterisation, and Electrochemical Investigation

Ying Tang,[a] Zhenhong Wei,[a] Wei Zhong,[a] and Xiaoming Liu*[a,b]

Keywords: [FeFe]-hydrogenases / Enzyme models / Iron / Bridging ligands / Electrochemistry / Reduction

Four diiron hexacarbonyl complexes, $[Fe_2(\mu\text{-}SCH_2\text{-}o\text{-}C_6H_4OMe)_2(CO)_6]$ (**4a**), $[Fe_2\{\mu\text{-}SCH_2\text{-}o,m\text{-}C_6H_3(OMe)_2\}_2(CO)_6]$ (**4b**), $[Fe_2\{\mu\text{-}SCH_2\text{-}o,o'\text{-}C_6H_3(CO_2Me)(OMe)\}_2(CO)_6]$ (**4c**) and the demethylated form of complex **4a**, $[Fe_2(\mu\text{-}SCH_2\text{-}o\text{-}C_6H_4OH)_2(CO)_6]$ (**5a**), were synthesised and fully characterised. Complexes **4b** and **4c** were also structurally analysed. Electrochemical investigations revealed that the integrity of the bridging linkages of the examined diiron complexes significantly affect their reduction reversibility and catalysis through a coupled chemical reaction in a unique ECE mechanism, widely adopted by complexes with the core $\{Fe_2(CO)_{4-6}\}$. Demethylation of complexes **4a** and **1**Me, $[Fe_2(\mu\text{-}SCH_2)_2CMe(CH_2\text{-}o\text{-}C_6H_4OMe)(CO)_6]$, by BBr_3 led to complexes (**5a** and **1**H, $[Fe_2(\mu\text{-}SCH_2)_2CMe(CH_2\text{-}o\text{-}C_6H_4OH)(CO)_6]$) with pendant phenol group(s), a weak acid. Deprotonation of the two complexes produced the pendant phenolate, which instantly intramolecularly substitutes the bound CO to yield species of the coordination form Fe^I–OR (R = phenolic moiety). Electrochemical investigation revealed that the pendant phenol groups in complexes **1**H and **5a** do not seem to improve their catalytic efficiency in proton reduction in the medium acetic acid/dichloromethane.

Introduction

Hydrogen is a potential energy vector, which is clean and carbon-free since its "combustion" produces only energy without by-products but only water. From water hydrogen could be regenerated at the expense of solar energy under the catalysis of hydrogenases as demonstrated by the principle possessed by photosystem II (PSII). This would be an ideal scenario, sustainable, renewable, and environmentally benign, which is undoubtedly what mankind would like to ideally achieve for our future. [FeFe]-hydrogenase is one of the two metalloenzymes existing in nature, capable of reversibly and rapidly catalysing hydrogen evolution and oxidation.[1] The crystal structures of the metalloenzymes isolated from *Desulfovibrio desulfuricans* and *Clostridium pasteurianum*, respectively, were revealed a decade ago.[2,3] The active site, H-cluster, is composed of one {4Fe4S}-cubane and one {2Fe2S}-subunit, Figure 1. The two iron atoms are bridged by a dithiolate ligand, whose true nature is still under debate,[2–5] and further coordinated by carbonyl and cyanide ligands. On the distal iron atom is located the binding site for a substrate, occupied by an exogenous ligand, H_2O or OH^- in its resting state, Figure 1.

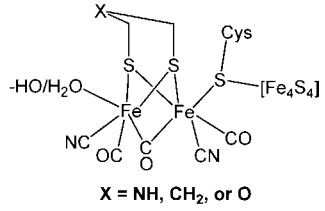

Figure 1. The H-cluster of [FeFe]-hydrogenase.

Since the revelation of the detailed structural information of the enzyme, mimicking of the diiron centre has attracted tremendous attention because of the relevance of hydrogen to energy, and a good collection of model complexes containing either a {2Fe2S} or {2Fe3S} core have been reported.[6–15] Some of those reported synthetic analogues duplicated delicately key structural features found in the H-cluster.[16–18] But attempts of preparing models to mimic the bonding feature Fe–OH_2(OH^-) had not been successful[19–23] because such a bond is doomed to be labile as it is necessary for this bond to be readily cleaved for substrate binding in the enzymatic catalysis. Indeed, we recently reported a model complex, $[Fe_2(\mu\text{-}SCH_2)_2CMe(CH_2\text{-}o\text{-}C_6H_4OH)(CO)_6]$ (**1**H), which bears a pendant phenol group, Scheme 1.[24] Deprotonation of the pendant phenol group led to an unstable diiron pentacarbonyl complex

[a] Department of Chemistry / Institute for Advanced Study, Nanchang University
Nanchang 330031, China
Fax: +86-791-3969254
E-mail: xiaoming.liu@ncu.edu.cn
[b] College of Biological, Chemical Sciences and Engineering, Jiaxing University
Jiaxing 314001, China
Fax: +86-573-83643937
E-mail: xiaoming.liu@mail.zjxu.edu.cn
Supporting information for this article is available on the WWW under http://dx.doi.org/10.1002/ejic.201001092.

whose identity was established by FTIR, tandem mass spectrometry and DFT calculations. This was the first example of a model possessing a Fe^{I}–OR (R = phenol moiety) bond.

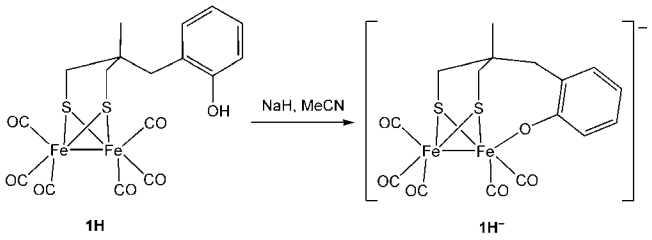

Scheme 1. Deprotonation of complex **1**H and the formation of complex **1**H$^-$.[24]

Herein, we report four diiron model complexes, [Fe_2(μ-SCH_2-*o*-$C_6H_4OMe)_2(CO)_6$] (**4a**), [Fe_2{μ-SCH_2-*o*,*m*-C_6H_3-$(OMe)_2$}$_2(CO)_6$] (**4b**), [Fe_2{μ-SCH_2-*o*,*o*′-$C_6H_3(CO_2Me)$-(OMe)}$_2(CO)_6$] (**4c**) and [Fe_2(μ-SCH_2-*o*-$C_6H_4OH)_2(CO)_6$] (**5a**), of which the last complex also possesses two pendant phenol groups. All the complexes were fully characterised and complexes **4b**, **4c** and **5a** were also crystallographically analysed. Deprotonation of complex **5a** produced a species that may have the two phenolate groups coordinated to the two iron atoms, [Fe_2(μ-SCH_2-*o*-$C_6H_4O)_2(CO)_4]^{2-}$ (**6a**), as suggested by its infrared spectrum. These complexes in addition to two complexes (**1**Me and **1**H) reported previously[24] were further electrochemically investigated to probe how the bridging linkage affects the ECE mechanism adopted widely by complexes with a core ({$Fe_2(CO)_{4-6}$}) in their electron transfer and whether a pendant phenol, a weak acid, would exert any influence on the catalytic reduction of a proton.

Results and Discussion

Synthesis

Complexes **4a**–**c** were prepared from the reaction of [Fe_2(μ-$S)_2(CO)_6$], which was prepared following the literature procedure,[25] with organic bromides (Schemes 2 and

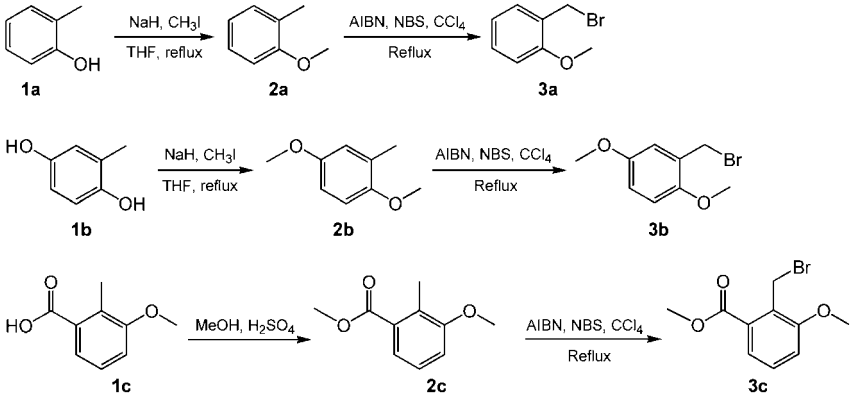

Scheme 2. Synthesis of the bromides bearing methoxy groups.

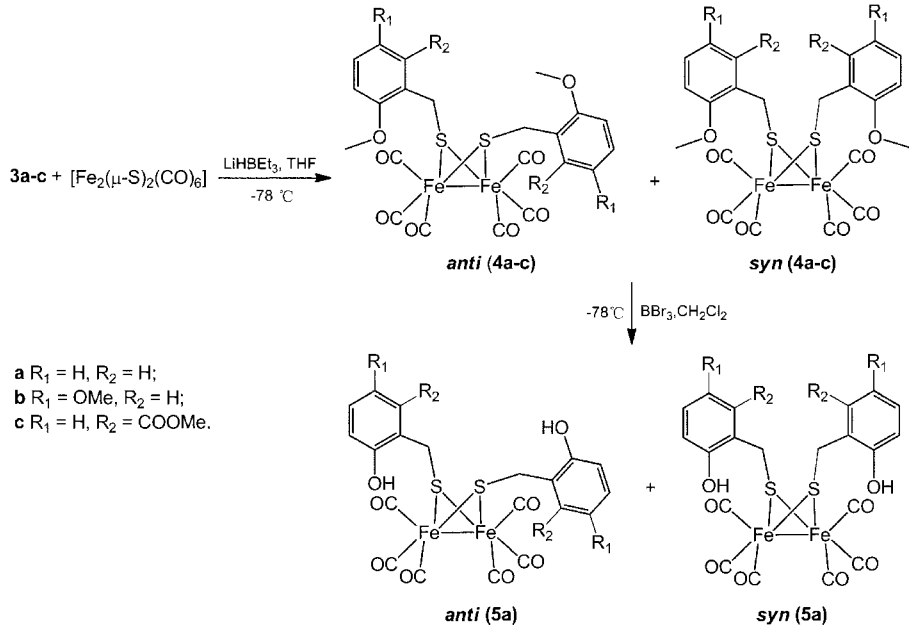

Scheme 3. Synthesis of complexes **4a**–**c** and **5a**.

3). As show in Scheme 2, the three aromatic bromides were prepared by bromination of derivatives of methylanisol. In these complexes, the phenyl moiety is linked to the dimetallic centre with a methylenethiolate. All the diiron complexes possess six carbon monoxide ligands and show characteristic spectral absorption bands of diiron hexacarbonyl complexes, Table 1. Unlike complex **1**H in which the bridging linkage is a dithiolate,[24] the diiron centre in complexes **4a**–**c** is bridged by two identical monothiolates. Therefore, the organic moieties of the two thiolates can take three possible conformations, *syn*, *syn′*, and *anti*, as observed widely in their analogues.[26–29] In the first conformation, both phenyl rings point away from the diiron centre. The opposite conformation is the *syn′* form, but it is thermodynamically unfavoured and hardly observed. The most thermodynamically stable form is the *anti* conformation. The distribution of the two conformations depends on the nature of the organic moiety. The ^{1}H NMR signals of the methylene groups in the spectra of these complexes can be used to determine the ratio of the two forms (*anti*/*syn*). For complexes **4a**, **4b** and **4c**, the ratios are approximately 8:1, 6:1 and 2:1, respectively. Apparently, the *anti* form in complex **4c** is more stable relative to those in the other two complexes. This can probably be attributed to the bulkiness of the bridging linkage contributed by the acylmethyl ester as shown in Scheme 2.

Table 1. Infrared absorption bands [cm^{-1}] of complexes **4a**–**c**, **5a** and **6a**.

Complex	υ_{CO}
4a	2069.2, 2033.5, 1991.8
4b	2069.8, 2033.9, 1993.3
4c	2068.6, 2032.9, 1990.8
5a	2070.9, 2035.9, 1994.6
1Me[a]	2072.9, 2032.5, 1999.7, 1990.2
1H[a]	2073.4, 2032.9, 2000.2, 1990.7
6a[b]	2020.8, 1993.4, 1944.0, 1909.7

[a] Adopted from ref.[24] [b] In acetonitrile.

By employing the same strategy as we described previously, we used BBr_3 to demethylate complexes **4a**–**c**, but only complex **5a** was obtained in a moderate yield.

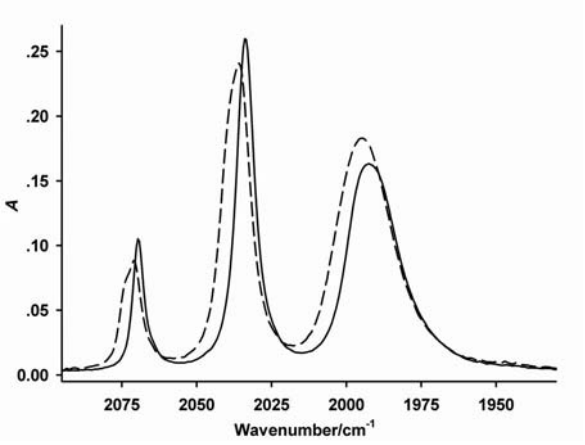

Figure 2. Infrared spectra of complex **4a** (solid line) and its demethylated product **5a** (dashed line).

Attempts to prepare complexes **5b** and **5c** were unsuccessful because of the difficulty in purifying the demethylated products. Complexes **4a** and **5a** show the same spectral envelope with a 2 cm^{-1} "blue" shift after demethylation (Figure 2). This small shift in the infrared absorption bands results from the replacement of the methoxy group by a hydroxy group in the conversion from complexes **4a** to **5a**. But the replacement occurs on the phenyl ring and is far away from the diiron centre, and thus the resultant electronic effect is rather limited.[24] As in complex **4a**, its demethylated product **5a** possesses two isomers at a rather similar ratio to that in complex **4a**.

Crystallographic Analysis

Diffusion of hexanes into a dichloromethane solutions of complexes **4b** and **4c** and storing of the mixtures at –20 °C for several days afforded dark red crystals of complexes **4b** and **4c** suitable for X-ray single crystal diffraction analysis. Their selected bond lengths and angles are tabulated in Table 2. Figure 3 shows the structural views of the two complexes. Geometries of these complexes show no drastic differences from currently existing diiron hexacarbonyl analogues. Crystals for complex **5a** were also crystallised in a

Table 2. Selected bond lengths [Å] and angles [°] of complexes **4b** and **4c**.

Complex	**4b**	**4c**
Fe1–Fe2	2.5174(5)	2.5224(14)
Fe1–S1	2.2726(5)	2.2624(17)
Fe1–S2	2.2570(5)	2.2550(18)
Fe2–S1	2.2706(5)	2.262(2)
Fe2–S2	2.2683(5)	2.2491(17)
Fe1–C1	1.7990(18)	1.815(6)
Fe1–C2	1.7893(18)	1.773(5)
Fe1–C3	1.7954(17)	1.792(5)
Fe2–C4	1.815(2)	1.781(6)
Fe2–C5	1.7883(18)	1.793(5)
Fe2–C6	1.788(2)	1.819(6)
C2–Fe1–C3	99.22(8)	90.8(2)
C2–Fe1–C1	91.10(8)	97.6(2)
C3–Fe1–C1	99.11(8)	100.1(2)
C2–Fe1–S2	91.25(6)	94.42(16)
C3–Fe1–S2	102.75(6)	156.79(17)
C1–Fe1–S2	157.34(6)	101.57(16)
C2–Fe1–S1	157.97(6)	156.07(18)
C3–Fe1–S1	102.61(6)	85.62(16)
C1–Fe1–S1	88.34(6)	106.29(18)
S2–Fe1–S1	81.167(19)	80.50(6)
S2–Fe1–Fe2	56.414(16)	55.83(5)
S1–Fe1–Fe2	56.313(13)	56.12(5)
C5–Fe2–C6	90.68(9)	103.3(2)
C5–Fe2–C4	97.26(9)	92.1(2)
C6–Fe2–C4	99.77(10)	98.6(3)
C5–Fe2–S2	93.80(6)	156.61(17)
C6–Fe2–S2	158.20(7)	98.63(17)
C4–Fe2–S2	100.80(6)	92.64(16)
C5–Fe2–S1	157.81(6)	87.26(16)
C6–Fe2–S1	86.86(7)	100.77(18)
C4–Fe2–S1	104.90(6)	160.2(2)
S2–Fe2–S1	80.97(2)	80.62(6)
S2–Fe2–Fe1	55.987(11)	56.05(5)
S1–Fe2–Fe1	56.388(15)	56.12(5)

similar procedure to give **5a**·0.25CH_2Cl_2. But its poor quality gave no satisfactory results in the structure refinements (Table S1 and Figure S1). Nevertheless, an approximate structure was generated, and the structural information revealed that it is essentially analogous to the other two complexes.

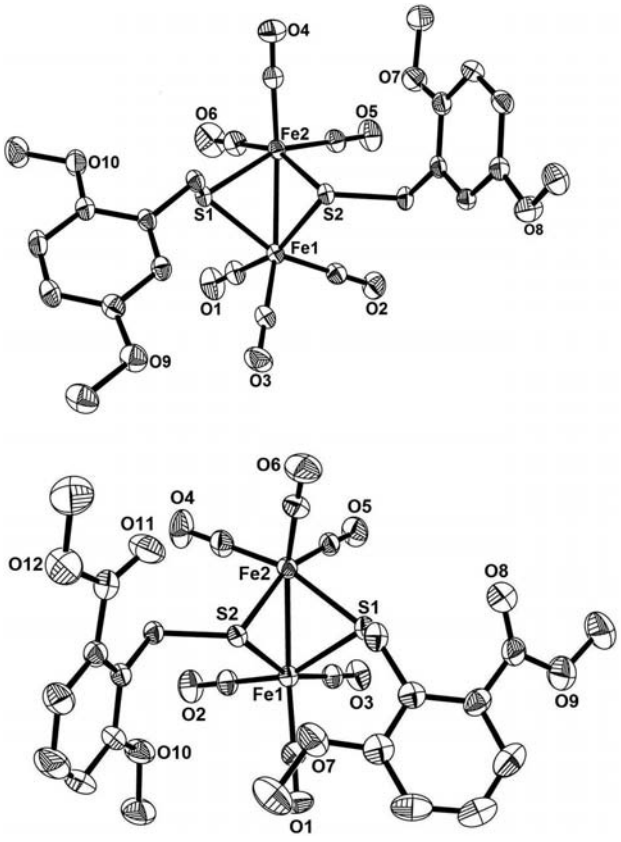

Figure 3. Crystal structures of model complexes **4b** (top) and **4c** (bottom) with ellipsoids drawn at a thermal probability of 50% (hydrogen atoms were omitted for clarity reasons).

Coordination of the Phenol Groups in Complex 5a to the Diiron Centre Upon Deprotonation

In our previous report, deprotonation of complex **1**H led to the formation of a monoanionic diiron pentacarbonyl complex with a bond between Fe^I and the phenolate.[24] Complex **5a** was treated in the same manner in acetonitrile and a group of neat absorption bands were observed, Figure 4, which accompanied a distinct colour change upon deprotonation from yellow–brown to dark red. Upon addition of an acid (HBF_4·Et_2O) under Ar, about 30% of the parent complex was recovered as estimated from the intensities of the infrared absorption bands, Figure 4. Close inspection of the spectral profile of the product reveals a similarity to those of diiron tetracarbonyl complexes.[23,30–32] Relative to the absorption bands of the parent complex **5a**, the absorption bands of the formed product are shifted to lower frequencies by about 85 cm^{-1} on average. This is comparable to those analogous shifts found for the conversion from hexacarbonyl to tetracarbonyl. By considering the partial recovery of the parent complex and the spectral features of the product upon deprotonation, it is assumed that the two pendant phenolates bind to the diiron centre, probably in a manner shown in Scheme 4. The structure proposed is based on the facts that the *anti* form is dominant in complexes of this type and that it is not unprecedented that one of the phenolate groups coordinates the iron atom in a basal position rather than in an axial position.[26,33] Plotting the absorption bands of a known diiron tetracarbonyl complex against the bands of the product produces a linear correlation (Figure S2), which serves as further support for the proposed tetracarbonyl product. Despite our attempts at using bulky organic cations, for example, Ph_4PBr or But_4NBF_4, isolating this product was not successful because of its instability as we observed previously for the monophenolate analogue.[24]

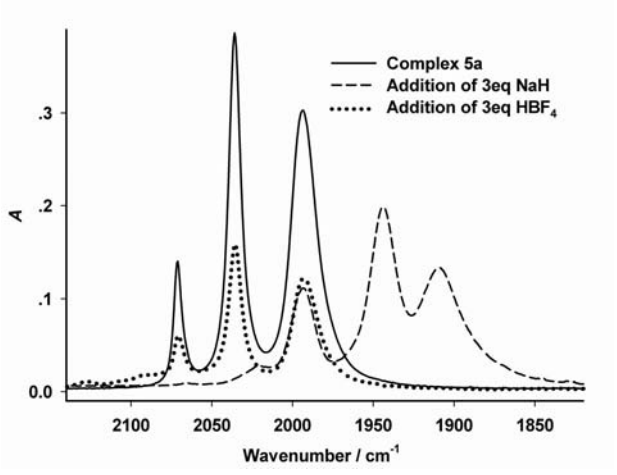

Figure 4. Infrared spectral variations for the interconversion from complex **5a** (solid line) to the product (presumably **6a**) (dashed line) and its partial recovery after acidification (dotted line).

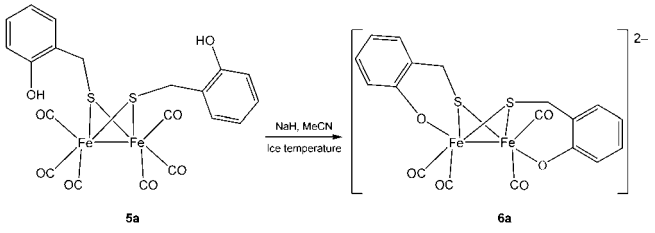

Scheme 4. Deprotonation of the pendant phenol groups and their possible binding modes to the two iron atoms.

Influence of Substituents of the Phenyl Rings in the Complexes (4a–c, 5a, 1Me, and 1H) on Their Electrochemical Behaviour

It is well understood that the reduction of complexes possessing the core $\{Fe_2(CO)_n\}$ (n = 4–6) is an ECE process but often appears with one reduction peak or with the second reduction potential slightly more negative than the first.[23,28,34–35] Indeed, the reduction of the complexes in-

vestigated here followed the proposed ECE mechanism when ferrocene was used as an external standard (data not shown). On the other hand, the redox behaviour of the complexes depends very much on the nature of the bridging linkage of the diiron centre. The complexes examined in this work fall into two categories, that is, complexes **1**Me and **1**H is in one group, while complexes **4a**–**c** and **5a** are in the other. Furthermore, complexes **1**H and **5a** possess pendant phenol groups, whereas in complexes **1**Me and **4a**–**c**, these phenols are methylated. The variation of these bridging linkages in both bulkiness and whether the two bridging thiolates are from an integrated multidentate ligand or two monothiolates makes these diiron complexes suitable for investigating the correlation between their electrochemical properties and the bridging moieties. Particularly, the pendant phenol group shows structural flexibility in its ability to coordinate to the diiron centre upon deprotonation as discussed above. Therefore, the pairs of complexes **1**Me/**1**H and **4a**/**5a** can be appropriate systems to examine how the pendant phenol group affects their electrochemical reduction and hence their catalysing proton reduction, i.e., whether this internal weak acid (pendant phenol) plays any role in the catalysis of proton reduction. Such a correlation would have particular interest with regard to guiding the designing and assembling of novel artificial analogues for the subunit of the [FeFe]-hydrogenase.

Because some of the complexes are not sufficiently soluble in acetonitrile, all the complexes, **4a**–**c**, **5a**, **1**Me and **1**H were electrochemically examined in dichloromethane, and their redox potentials are tabulated in Table 3. Their redox processes are shown in Figures 5 and S3. In general, the redox potentials are related to the capability of electron donation of the bridging linkages. It is interesting to note the difference between the reduction peak potential and the oxidation peak potential of the investigated complexes, $^{red}E_c - {}^{ox}E_a$, as shown in Table 3. The potential differences are significantly affected by the replacement of a methoxy group by a hydroxy group and much less by the variation in the bridging linkages, although fluctuations in both reduction and oxidation potentials with the linkages are obvious. For complexes **4a**–**c** and **1**Me, the potential difference is about 2.3 V, whereas for complexes **5a** and **1**H, which were derived from demethylation of their parent complexes, the potential difference is about 2.1 V. Since reduction and oxidation potentials are directly correlated to the energy levels of HOMO and LUMO of a molecule, respectively, these observations imply that the hydroxy groups decrease the energy gap between the frontier orbitals more than that observed for the non-hydroxy groups. It is certain that the hydroxy groups electronically influence the redox potentials, but exactly how the hydroxy groups exert the influence on the frontier orbitals is hard to explain without further theoretical exploration.

Table 3. Redox potentials [V] of complexes **4a**–**c**, **5a**, **1**Me and **1**H in dichloromethane.

Complex	Reduction, E_c/E_a	Oxidation, E_a[a]	$^{red}E_c - {}^{ox}E_a$
4a	–1.656[b]	0.629	–2.29
4b	–1.618[b]	0.731	–2.35
4c	–1.740[b]	0.596	–2.34
5a	–1.501[b]	0.635, 0.879[c]	**–2.14**
1Me	–1.550/–1.477	0.857	–2.33
1H	–1.508/–1.386	0.767	**–2.15**

[a] Irreversible oxidation. [b] Irreversible reduction. [c] From a daughter product and is not used in the calculation of the potential difference.

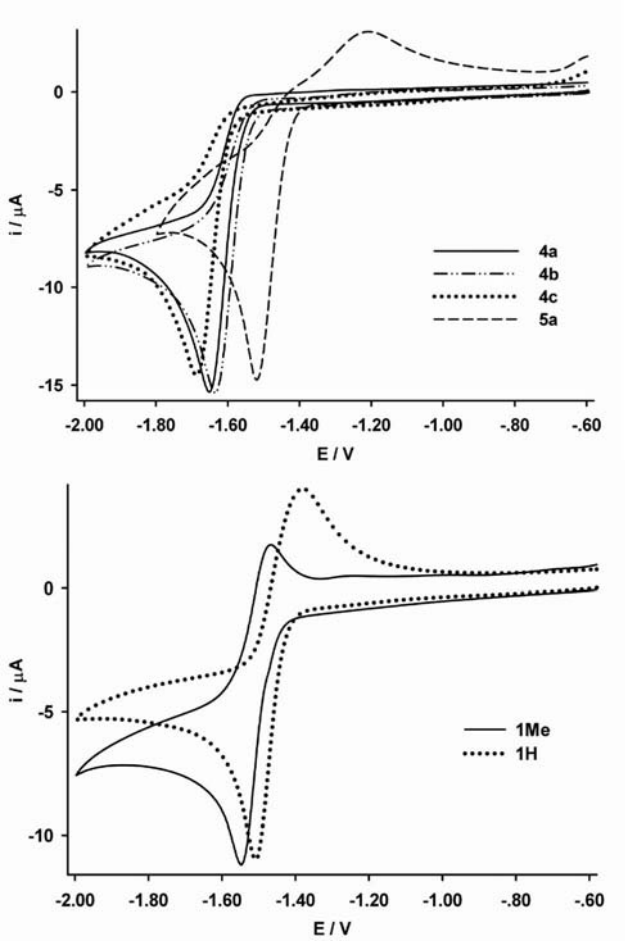

Figure 5. Reduction behaviour of complex **4a**–**c**, **5a** (top) and **1**Me and **1**H (bottom) in dichloromethane (scan rate = 0.1 $V s^{-1}$, 298 K).

The bridging linkages of the complexes not only exert an electronic influence on the redox potentials, but also affect the reversibility of the reduction processes. As shown in Figure 5, under the same conditions, complexes **1**Me and **1**H exhibit decent reversibility, whereas for the others, no reversibility was observed. As mentioned earlier, the reduction of the diiron complexes follows a unique ECE mechanism. The results observed in this work further shed some light on the nature of the coupled chemical reaction. It seems that one of the two bridging thiolate groups might entirely de-coordinate in this chemical reaction. If this is the case, the fact that the reversibility varies with the bridging linkage can be explained. In complexes **1**Me and **1**H, the dithiolate that bridges the two iron atoms is an integrated bidentate ligand, which allows the de-coordinated

thiolate to dangle around and re-coordinate to the metal centre when necessary. However, in the other complexes, such a de-coordination would lead to a permanent departure of the de-coordinated thiolate group.

By considering the different reduction behaviours between the two categories of diiron complexes (Figure 5), it is not surprising that they respond rather differently upon the addition of an acid (acetic acid). Figure 6 shows the catalytic reduction of a proton by complex **4a**. As suggested by their cyclic voltammograms (Figures S4 and S5), the catalysis of the other two analogues (**4b** and **4c**) is essentially similar to that of complex **4a**. For complex **1**Me, catalysis occurs at a potential more negative by ca. 300 mV relative to the reduction potential of the first process, which is hardly affected by the addition of the acid (Figure 7). This is rather different from the catalysis by complexes **4a**–**c** (Figures 6, S4 and S5). The experimental observations support the suggestion that the monoanion generated from the first one-electron reduction is not responsible for the catalysis.[23] The striking difference in catalytic potentials for the two categories of complexes is thought to be associated with the difference in the chemical reaction coupled with the electron-transfer process as discussed above.

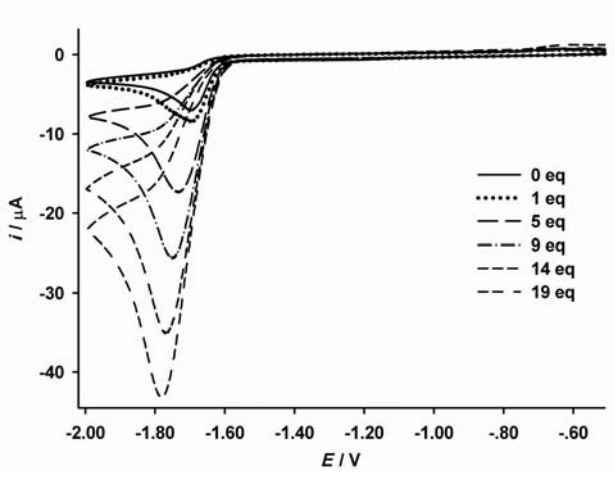

Figure 6. Cyclic voltammograms of complex **4a** (C = 3.30 mmol L^{-1}) without and with the addition of acetic acid in dicholormethane (scan rate = 0.1 V s^{-1}, 298 K).

As indicated by the redox potentials in Table 3, demethylation causes noticeable variation in the energies of the frontier orbitals for the pairs of complexes **4a** and **5a**, **1**Me and **1**H. However, with regard to their catalysis, no essential difference is observed for these complexes (Figures 6, 7, S6 and S7). The only noticeable difference observed is the neat cyclic voltammograms observed for the complexes without pendant phenol groups (**4a**–**c** and **1**Me). This can probably be attributed to the adsorbing preference on the surface of a vitreous carbon electrode possessed by species with phenol groups as the surface of a vitreous carbon electrode is rich in functional groups, for instance, hydroxy and carboxylic groups. However, the presence of a pendant phenol group does not lead to a significant change in the catalytic efficiency of proton reduction (Figures S8 and S9).

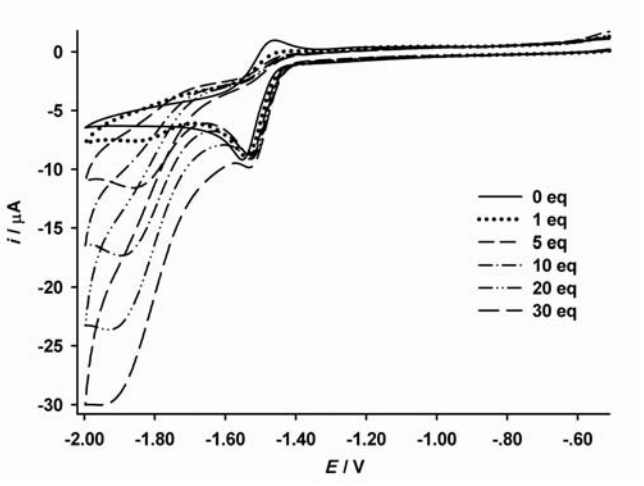

Figure 7. Cyclic voltammograms of complex **1**Me (C = 3.24 mmol L^{-1}) without and with the addition of the acid in dichloromethane (scan rate = 0.1 V s^{-1}, 298 K).

Conclusions

In this work, four diiron hexacarbonyl complexes, **4a**–**c** and **5a**, in addition to two complexes **1**Me and **1**H reported previously,[24] were investigated electrochemically without and with the presence of acetic acid in dichloromethane. These complexes are believed to adopt the unique ECE mechanism for electron transfer, in which the potential for the second reduction could be either more positive or marginally more negative than the first one. Our results also show that the bridging linkages of the diiron complexes significantly affect the chemical reaction coupled to the first electron-transfer process. When the two thiolate groups are from two monothiolates, the coupled chemical reaction may be associated with the partial deconstruction of the diiron moiety, for example, the permanent cleavage of one of the two thiolates. Such a destruction is much less significant for complexes **1**Me and **1**H, as suggested by their quasireversible reductions; the bidentate ligand certainly made the difference. Demethylation of complexes **4a** and **1**Me led to complexes (**5a** and **1**H) with pendant phenol group(s). However, this pendant weak acid does not seem to exert much influence on the catalysis of proton reduction.

Experimental Section

General Procedures: All reactions were carried out under an argon atmosphere by using standard Schlenk technique. Solvents for reactions and electrochemistry were freshly distilled by using appropriate drying agents prior to use. Infrared spectroscopic data were collected on a Scimitar 2000 (Varian) instrument in an appropriate solvent by using a solution cell (spacer = 1 mm). NMR spectra were recorded on an Avance DRX-400 or–600 (Bruker) instrument. Electrochemistry was performed as described elsewhere.[23,28,33,36] All potentials were quoted against the ferrocenium/ferrocene couple, F_C^+/F_C. The microanalysis service was provided by the Centre of Analysis and Testing at Nanchang University and Nanjing University.

Synthesis

Preparation of $[Fe_2(\mu\text{-}S)_2(CO)_6]$: After being flushed with Ar, a three-necked round-bottomed flask (1 L) was charged with $Fe(CO)_5$ (25 mL, 186 mmol), followed by dry MeOH (125 mL) and finally freshly prepared aqueous KOH (75 mL, 75%). After stirring for 30 min, the homogeneous solution was cooled to ice temperature in an ice bath, and then S_8 (33 g, 1.03 mol) was slowly added. After the addition and further stirring for 1 h, the reaction mixture was treated with H_2O (250 mL), hexanes (150 mL), and finally NH_4Cl (85 g, 1.6 mol). The ice bath was then removed, and the reaction solution was stirred at room temperature for an additional 16 h. The reaction mixture was then extracted with petroleum ether (4 × 200 mL). The extracts were combined, and the solvents were removed to give a crude product, which was purified by using flash chromatography (eluent: petroleum ether) to produce a red solid (9.7 g, 30%). Mp: 46–47 °C. IR [acetonitrile]: ν_{CO} = 2084.0, 2041.8, 2002.7 cm^{-1}.

Synthesis of 2-Methylanisol, 2a: A stirred suspension of NaH (6.0 g, 150 mmol, 60% dispersion in mineral oil) in dry THF (120 mL) was cooled to ice temperature in an ice bath. To the suspension was slowly added a solution of *o*-cresol (**1a**, 10.8 g, 100 mmol) in dry THF (20 mL). When there was no more hydrogen gas evolving, CH_3I (7.2 mL, 115 mmol) was added dropwise. The reaction mixture was warmed to 85 °C and stirred overnight. Completion of the reaction was confirmed by using TLC (petroleum ether/ethyl acetate = 10:1). After removal of the solvent, water (50 mL) was added. After extraction with ethylacetate (3 × 50 mL) and purification by column chromatography (petroleum ether/ethyl acetate, 10:1), the desired compound was obtained as a colourless liquid (11.8 g, 97%). ^1H NMR ($CDCl_3$, 400 MHz): δ = 7.16 (m, 2 H, Ar*H*), 6.84 (m, 2 H, Ar*H*), 3.82 (s, 3 H, OCH_3), 2.22 (s, 3 H, CH_3) ppm.

Synthesis of 1,4-Dimethoxy-2-methylbenzene, 2b: Compound **2b** was synthesised in the same procedure as described above for compound **2a** by using 2-methylhydroquinone (6.3 g, 50 mmol), NaH (6 g, 150 mmol, 60% dispersion in mineral oil) and CH_3I (10 mL, 150 mmol). It was isolated as a colourless liquid (6.8 g, 88%). ^1H NMR ($CDCl_3$, 400 MHz): δ = 6.59–6.69 (m, 3 H, Ar*H*), 3.69 (s, 3 H, OCH_3), 3.66 (s, 3 H, OCH_3), 2.18 (s, 3 H, CH_3) ppm.

Synthesis of Methyl(3-methoxy-2-methyl)benzoate (2c): 3-Hydroxy-2-methylbenzoic acid (**1c**, 3.2 g, 20 mmol) was dissolved in dry MeOH (20 mL, 500 mmol) and mixed with concentrated H_2SO_4 (2 mL, 35.5 mmol, 95%). The solution was heated at reflux overnight. Removal of the solvents gave a residue to which water (30 mL) was then added. Extraction with ethyl acetate (3 × 30 mL) and routine work-up gave compound **2c** as a colourless liquid (3.3 g, 95%) without further purification for the next reaction. ^1H NMR ($CDCl_3$, 400 MHz): δ = 7.30 (d, J = 7.76 Hz, 1 H, Ar*H*), 7.07 (t, J = 7.98 Hz, 1 H, Ar*H*), 6.86 (d, J = 8.12 Hz, 1 H, Ar*H*), 4.53 (s, 2 H, CH_2), 3.77 (s, 3 H, COOCH_3), 3.71 (s, 3 H, OCH_3), 2.33 (s, 3 H, CH_3) ppm.

Synthesis of 2-Bromomethylanisol (3a): A solution of compound **2a** (7.3 g, 60 mmol), NBS (10.7 g, 60 mmol) and AIBN (160 mg, 1 mmol) in CCl_4 (250 mL) was heated at reflux for about 1 h until a white solid was floating on the surface. The mixture was filtered, and the filtrate was then concentrated under reduced pressure to produce a residue. Recrystallisation of the residue in hexanes afforded a white solid (11.5 g, 93%). Mp: 47–50 °C. ^1H NMR ($CDCl_3$, 600 MHz): δ = 7.30 (m, 2 H, Ar*H*), 6.93 (m, 1 H, Ar*H*), 6.88 (m, 1 H, Ar*H*), 4.57 (s, 2 H, 2 × CH*H*), 3.88 (s, 3 H, OCH_3) ppm. ^{13}C NMR ($CDCl_3$, 600 MHz): δ = 157.45, 130.89, 130.21, 126.07, 120.67, 110.95, 55.57, 29.06 ppm.

Synthesis of 1,4-Dimethoxy-2-bromomethylbenzene (3b): Compound **3b** was prepared by following the same experimental procedure described for compound **3a** by using compound **2b** (6.1 g, 40 mmol), NBS (7 g, 40 mmol) and AIBN (160 mg, 1 mmol). The compound was obtained as a needle-shaped crystalline solid (8.5 g, 92%). Mp: 71–73 °C. ^1H NMR ($CDCl_3$, 600 MHz): δ = 6.89 (d, J = 2.4 Hz, 1 H, Ar*H*), 6.79–6.83 (m, 2 H, Ar*H*), 4.53 (s, 2 H, CH_2), 3.84 (s, 3 H, OCH_3), 3.76 (s, 3 H, OCH_3) ppm.

Synthesis of Methyl(3-methoxy-2-bromomethyl)benzoate (3c): The same procedure was adopted to produce compound **3c** as a white solid (4.5 g, 96%) by using compound **2c** (3.3 g, 18 mmol), NBS (3.3 g, 18 mmol) and AIBN (60 mg, 0.4 mmol) in CCl_4 (160 mL). Mp: 112–114 °C. ^1H NMR ($CDCl_3$, 600 MHz): δ = 7.05 (m, 1 H, Ar*H*), 7.32 (t, J = 8.1 Hz, 1 H, Ar*H*), 7.06 (d, J = 8.4 Hz, 1 H, Ar*H*), 5.0 5 (s, 2 H, CH_2), 3.92 (s, 3 H, COOCH_3), 3.91 (s, 3 H, OCH_3) ppm.

Synthesis of $[Fe_2(\mu\text{-}SCH_2\text{-}o\text{-}C_6H_4OMe)_2(CO)_6]$ (4a): A solution of $[Fe_2(\mu\text{-}S)_2(CO)_6]$ (1.2 g, 3.5 mmol) in dry THF (60 mL), precooled to –78 °C with a dry-ice/acetone bath, was treated with $LiBHEt_3$ (7 mL, 1 mol L^{-1} in dry THF). After stirring the mixture for 30 min, compound **3a** (1.4 g, 7.0 mmol) was added. The mixture was stirred at –78 °C for 30 min and was then warmed to room temperature for an additional 2 h. Removal of the solvent produced a crude product, which was purified by using flash chromatography (petroleum ether/ethyl acetate, 20:1) to give a red solid (1.6 g, 78%). Mp: 141–142 °C. IR [dichloromethane]: ν_{CO} = 2069.2, 2033.5, 1991.8 cm^{-1}. ^1H NMR ($CDCl_3$, 400 MHz): δ = 6.77–7.33 (m, 9 H, Ar*H*, *anti*/*syn* ratio 8:1), 3.94 (s, 3 H, *anti*-OCH_3), 3.84 (s, 0.75 H, *syn*-OCH_3), 3.71 (s, 3 H, *anti*-OCH_3), 3.67 (s, 2 H, *anti*-CH_2), 3.61 (s, 0.5 H, *syn*-CH_2), 3.25 (s, 2 H, *anti*-CH_2) ppm. $C_{22}H_{18}Fe_2O_8S_2$ (586.19): calcd. C 45.08, H 3.10; found C 44.94, H 3.29.

Synthesis of $[Fe_2\{\mu\text{-}SCH_2C_6H_3(OMe)_2\}_2(CO)_6]$ (4b): Complex **4b** was prepared from $[Fe_2(\mu\text{-}S)_2(CO)_6]$ (1.05 g, 3 mmol), $LiBHEt_3$ (6 mL, 1 M in dry THF) and compound **2b** (1.5 g, 6 mmol) following the same procedure used to prepare complex **4a**. Complex **4b** was obtained as a red solid (1.2 g, 63%). Mp: 136–137 °C. IR [dichloromethane]: ν_{CO} = 2069.8, 2033.9, 1993.3 cm^{-1}. ^1H NMR ($CDCl_3$, 600 MHz): δ = 6.56–6.92 (m, 6 H, Ar*H*, *anti*/*syn* 6:1), 3.89 (s, 3 H, *anti*-OCH_3), 3.81 (s, 3 H, *anti*-OCH_3), 3.81 (s, 1 H, *syn*-OCH_3), 3.75 (s, 1 H, *syn*-OCH_3), 3.70 (s, 3 H, *anti*-OCH_3), 3.65 (s, 3 H, *anti*-OCH_3), 3.63 (s, 2 H, *anti*-CH_2), 3.58 (s, 0.63 H, *syn*-CH_2), 3.23 (s, 2 H, *anti*-CH_2) ppm. ^{13}C NMR ($CDCl_3$, 600 MHz): δ = 209.98, 208.86, 153.56, 153.46, 153.28, 151.61, 151.45, 151.28, 128.61, 127.98, 127.68, 116.45, 116.10, 115.77, 114.17, 113.96, 113.75, 111.78, 111.60, 111.54, 55.80.55.78, 55.70, 55.63, 55.56, 55.43, 38.28, 36.83, 31.60, 23.85 ppm. $C_{24}H_{22}Fe_2O_{10}S_2$ (646.26): calcd. C 44.60, H 3.43; found C 44.46, H 3.30.

Synthesis of $[Fe_2\{\mu\text{-}SCH_2C_6H_3(COOMe)OMe\}_2(CO)_6]$ (4c): Complex **4c** was synthesised as described for **4a** from $[Fe_2(\mu\text{-}S)_2(CO)_6]$ (1.2 g, 3.6 mmol), $LiBHEt_3$ (7 mL, 1 M in dry THF) and compound **3c** (1.8 g, 7 mmol) as a red solid (1.6 g, 65%). Mp: 174–176 °C. IR [dichloromethane]: ν_{CO} = 2068.6, 2032.9, 1990.8 cm^{-1}. ^1H NMR ($CDCl_3$, 600 MHz): δ = 7.56 (d, J = 7.2 Hz, 1 H, *anti*-Ar*H*), 7.46 (d, J = 7.2 Hz, 1 H, *syn*-Ar*H*), 7.37 (d, J = 7.2 Hz, 1 H, *anti*-Ar*H*), 7.33 (t, J = 7.8 Hz, 1 H, *anti*-Ar*H*), 7.25 (t, J = 9.6 Hz, 1 H, *syn*-Ar*H*), 7.21 (t, J = 7.8 Hz, 1 H, *anti*-Ar*H*), 7.10 (d, J = 8.4 Hz, 1 H, *anti*-Ar*H*), 7.00 (d, J = 7.8 Hz, 1 H, *syn*-Ar*H*), 7.90 (d, J = 8.4 Hz, 1 H, *anti*-Ar*H*), 4.07–4.64 (m, 24 H, PhCH_2, PhOCH_3, PhCOOCH_3 *anti*/*syn* 2:1) ppm. ^{13}C NMR ($CDCl_3$, 600 MHz): δ = 210.30, 209.11, 167.52, 167.43, 167.21, 157.79, 157.55, 157.45, 131.33, 130.57, 130.24, 129.74, 129.17, 128.52, 128.42, 128.35, 128.11, 122.89, 122.85, 122.59, 114.01, 113.83, 55.60, 55.51, 55.16,

52.29, 52.18, 52.12, 34.47, 32.35, 21.42 ppm. $C_{26}H_{22}Fe_2O_{12}S_2$ (702.28): calcd. C 44.47, H 3.16; found C 44.62, H 3.53.

Synthesis of [Fe_2(μ-SCH_2-*o*-$C_6H_4OH)_2(CO)_6$] (5a): To a precooled solution of [Fe_2(μ-$SCH_2C_6H_4OCH_3)_2(CO)_6$] (680 mg, 1.16 mmol) in dry dichloromethane (50 mL) in a dry-ice/acetone bath was added a solution of BBr_3 (1 mol L^{-1}, 5 mL) in dry dichloromethane under argon. After the addition, the reaction mixture was stirred at –78 °C for 2 h and then warmed to room temperature for an additional 6 h. The reaction mixture was cooled in an ice bath, and methanol (2 mL) was slowly added to quench the reaction. Removal of the solvents left a residue, which was purified by using flash chromatography in a gradient eluting manner (petroleum ether/ethyl acetate, 10:1, 8:1 and 5:1) to give a dark red solid (377 mg, 58.2%). Mp: 138 °C. IR [dichloromethane]: ν_{CO} = 2070.9, 2035.9, 1994.6 cm^{-1}. ^1H NMR ($CDCl_3$, 600 MHz): δ = 6.75–7.27 (m, 9 H, Ar*H*, *anti*/*syn* 8:1), 5.34 (s, 1 H, *anti*-PhO*H*), 5.25 (s, 1 H, *anti*-PhO*H*), 5.08 (s, 0.25 H, *syn*-PhO*H*), 3.70 (s, 2 H, *anti*-CH_2), 3.63 (s, 0.5 H, *syn*-CH_2), 3.26 (s, 2 H, *anti*-CH_2) ppm. $C_{20}H_{14}Fe_2O_8S_2$ (558.14): calcd. C 43.04, H 2.53; found C 42.65, H 2.71.

Deprotonation of Complex 5a: To NaH (60% in oil, 13.2 mg, 0.33 mmol) in a Schlenk tube precooled with an ice bath was added a solution of complex **5a** (40 mg, 0.079 mmol) in dry acetonitrile (5 mL) under rapid stirring. The colour of the solution changed quickly from yellow–brown to dark red. The reaction was complete within 2 h, as confirmed by infrared spectroscopic monitoring. IR [acetonitrile]: ν_{CO} = 2020.8, 1993.4, 1944.0, 1909.7 cm^{-1}.

X-ray Single-Crystal Diffraction: Standard procedures were used for mounting the crystals on a Bruker 98 APEX2 area-detector diffractometer at 296(2) K. The crystals were routinely wrapped with paraffin oil before being mounted. Intensity data were collected by using Mo-Ka radiation (λ = 0.71073 Å) under 296(2) K with a ϕ- and ω-scan mode. The SAINT and SADABS programs in the APPEX(II) software package were used for integration and absorption correction. The structures were solved by using direct methods with the SHELXS-97 program and refined on F^2 with XSHELL6.3.1; all non-hydrogen atoms were anisotropically modelled. All hydrogen atoms were geometrically positioned. Crystallographic details of these complexes are summarised in Table 4. CCDC-795447 (**4b**), -795448 (**4c**) and -795449 (**5a**) contain the supplementary crystallographic data for this paper. These data can be obtained free of charge from The Cambridge Crystallographic Data Centre via www.ccdc.cam.ac.uk/data_request/cif.

Table 4. Crystallographic data and processing parameters for complexes **4b**,**c**.

Complex	**4b**	**4c**
Empirical formula	$C_{24}H_{22}Fe_2O_{10}S_2$	$C_{26}H_{22}Fe_2O_{12}S_2$
F_w	646.26	702.28
T / K	296(2)	296(2)
Crystal system	triclinic	triclinic
Space group	$P\bar{1}$	$P\bar{1}$
a [Å]	8.9004(17)	11.018(8)
b [Å]	9.5959(18)	11.061(8)
c [Å]	17.285(4)	13.150(9)
a [°]	101.806(3)	88.948(8)
b [°]	95.464(3)	79.530(9)
c [°]	107.528(2)	70.571(8)
V / Å^3	1358.3(5)	1484.6(18)
Z	2	2
$q_{calcd.}$ / g cm^{-3}	1.580	1.571
F(000)	660	716
Reflections collected (unique)	12866(6842)	12625(7290)
Reflections [R_{int}]	6842(0.0170)	7290(0.0282)
Goodness-of-fit on F^2	1.017	1.073
Final R_1[a] [I > 2σ(I)]	0.0264	0.0583
Final wR_2[a]	0.0684	0.1350

[a] $R_1 = \Sigma||F_o| - |F_c||/\Sigma|F_o|$ and $wR_2 = [\Sigma(|F_o^2 - F_c^2|)^2/\Sigma(wF_o^2)^2]^{1/2}$.

Supporting Information (see footnote on the first page of this article): Crystallographic data, the structural view of complex **5a**, further spectroscopic data and cyclic voltammograms are included.

Acknowledgments

We thank the National Natural Science Foundation of China (Grant No. 20871064), the Ministry of Science and Technology (China) (973 program, Grant No: 2009CB220009), and the State Key Laboratory of Coordination Chemistry (Nanjing University, China) for supporting this work.

[1] D. J. Evans, C. J. Pickett, *Chem. Soc. Rev.* **2003**, *32*, 268–275.
[2] J. W. Peters, W. N. Lanzilotta, B. J. Lemon, L. C. Seefeldt, *Science* **1998**, *282*, 1853–1858.
[3] Y. Nicolet, C. Piras, P. Legrand, C. E. Hatchikian, J. C. Fontecilla-Camps, *Structure* **1999**, *7*, 13–23.
[4] U. Ryde, C. Greco, L. De Gioia, *J. Am. Chem. Soc.* **2010**, *132*, 4512–4513.
[5] B. E. Barton, M. T. Olsen, T. B. Rauchfuss, *J. Am. Chem. Soc.* **2008**, *130*, 16834–16835.
[6] X. M. Liu, S. K. Ibrahim, C. Tard, C. J. Pickett, *Coord. Chem. Rev.* **2005**, *249*, 1641–1652.
[7] F. F. Xu, C. Tard, X. F. Wang, S. K. Ibrahim, D. L. Hughes, W. Zhong, X. R. Zeng, Q. Y. Luo, X. M. Liu, C. J. Pickett, *Chem. Commun.* **2008**, 606–608.
[8] L. C. Song, G. H. Zeng, S. X. Lou, H. N. Zan, J. B. Ming, Q. M. Hu, *Organometallics* **2008**, *27*, 3714–3721.
[9] P. Li, M. Wang, L. Chen, J. H. Liu, Z. B. Zhaoa, L. C. Sun, *Dalton Trans.* **2009**, 1919–1926.
[10] B. E. Barton, M. T. Olsen, T. B. Rauchfuss, *Curr. Opin. Biotechnol.* **2010**, *21*, 292–297.
[11] P. Volkers, T. B. Rauchfuss, *J. Inorg. Biochem.* **2007**, *101*, 1748–1751.
[12] C. Tard, C. J. Pickett, *Chem. Rev.* **2009**, *109*, 2245–2274.
[13] M. L. Singleton, J. H. Reibenspies, M. Y. Darensbourg, *J. Am. Chem. Soc.* **2010**, *132*, 8870–8871.
[14] W. M. Gao, J. L. Sun, T. Akermark, M. R. Li, L. Eriksson, L. C. Sun, B. Akermark, *Chem. Eur. J.* **2010**, *16*, 2537–2546.
[15] S. Ezzaher, A. Gogoll, C. Bruhn, S. Ott, *Chem. Commun.* **2010**, *46*, 5775–5777.
[16] C. Tard, X. M. Liu, S. K. Ibrahim, M. Bruschi, L. De Gioia, S. C. Davies, X. Yang, L. S. Wang, G. Sawers, C. J. Pickett, *Nature* **2005**, *433*, 610–613.
[17] T. Liu, M. Y. Darensbourg, *J. Am. Chem. Soc.* **2007**, *129*, 7008–7009.
[18] C. M. Thomas, T. Liu, M. B. Hall, M. Y. Darensbourg, *Inorg. Chem.* **2008**, *47*, 7009–7024.
[19] P. I. Volkers, T. B. Rauchfuss, S. R. Wilson, *Eur. J. Inorg. Chem.* **2006**, 4793–4799.
[20] J. F. Capon, S. Ezzaher, F. Gloaguen, F. Y. Petillon, P. Schollhammer, J. Talarmin, T. J. Davin, J. E. McGrady, K. W. Muir, *New J. Chem.* **2007**, *31*, 2052–2064.
[21] C. M. Thomas, O. Rudiger, T. Liu, C. E. Carson, M. B. Hall, M. Y. Darensbourg, *Organometallics* **2007**, *26*, 3976–3984.
[22] A. K. Justice, T. B. Rauchfuss, S. R. Wilson, *Angew. Chem. Int. Ed.* **2007**, *46*, 6152–6154.
[23] Y. W. Wang, Z. M. Li, X. H. Zeng, X. F. Wang, C. X. Zhan, Y. Q. Liu, X. R. Zeng, Q. Y. Luo, X. M. Liu, *New J. Chem.* **2009**, *33*, 1780–1789.

[24] W. Zhong, Y. Tang, G. Zampella, X. Wang, X. Yang, B. Hu, J. Wang, Z. Xiao, Z. Wei, H. Chen, L. De Gioia, X. Liu, *Inorg. Chem. Commun.* **2010**, *13*, 1089–1092.
[25] J. L. Stanley, T. B. Rauchfuss, S. R. Wilson, *Organometallics* **2007**, *26*, 1907–1911.
[26] X. Zhao, Y. M. Hsiao, C. H. Lai, J. H. Reibenspies, M. Y. Darensbourg, *Inorg. Chem.* **2002**, *41*, 699–708.
[27] W. Zhong, G. Zampella, Z. M. Li, L. De Gioia, Y. Q. Liu, X. R. Zeng, Q. Y. Luo, X. M. Liu, *J. Organomet. Chem.* **2008**, *693*, 3751–3759.
[28] X. H. Zeng, Z. M. Li, Z. Y. Xiao, Y. W. Wang, X. M. Liu, *Electrochem. Commun.* **2010**, *12*, 342–345.
[29] X. Ru, X. H. Zeng, Z. M. Li, D. J. Evans, C. X. Zhan, Y. Tang, L. J. Wang, X. M. Liu, *J. Polym. Sci., Part A: Polym. Chem.* **2010**, *48*, 2410–2417.
[30] A. Le Cloirec, S. P. Best, S. Borg, S. C. Davies, D. J. Evans, D. L. Hughes, C. J. Pickett, *Chem. Commun.* **1999**, 2285–2286.
[31] X. Zhao, I. P. Georgakaki, M. L. Miller, R. Mejia-Rodriguez, C. Y. Chiang, M. Y. Darensbourg, *Inorg. Chem.* **2002**, *41*, 3917–3928.
[32] R. Mejia-Rodriguez, D. S. Chong, J. H. Reibenspies, M. P. Soriaga, M. Y. Darensbourg, *J. Am. Chem. Soc.* **2004**, *126*, 12004–12014.
[33] C. Zhan, X. Wang, Z. Wei, D. J. Evans, X. Ru, X. Zeng and X. Liu, *Dalton Trans.* **2010**, DOI: 10.1039/C1030DT00687D.
[34] G. A. N. Felton, C. A. Mebi, B. J. Petro, A. K. Vannucci, D. H. Evans, R. S. Glass, D. L. Lichtenberger, *J. Organomet. Chem.* **2009**, *694*, 2681–2699.
[35] J. F. Capon, F. Gloaguen, F. Y. Petillon, P. Schollhammer, J. Talarmin, *Coord. Chem. Rev.* **2009**, *253*, 1476–1494.
[36] Z. M. Li, X. H. Zeng, Z. G. Niu, X. M. Liu, *Electrochim. Acta* **2009**, *54*, 3638–3644.

Received: October 13, 2010
Published Online: January 11, 2011

